RADIATIVE RECOMBINATION DETECTION TO MONITOR ELECTRON COOLING CONDITIONS DURING LOW ENERGY RHIC OPERATIONS *

F. Carlier
CERN, Geneva, Switzerland and NIKHEF, Amsterdam, Netherlands
M. Blaskiewicz, A. Drees, A. Fedotov, W. Fischer,
M. Minty, C. Montag, G. Robert-Demolaize, P. Thieberger
BNL, Upton, NY 11973, USA

Abstract

Providing Au-Au collisions in the Relativistic Heavy Ion Collider (RHIC) at energies equal or lower than 10 GeV/nucleon is of particular interest to study the location of a critical point in the QCD phase diagram. To mitigate luminosity limitations arising from intra-beam scattering at such low energies, an electron cooling system is being developed. To achieve cooling, the relative velocities of the electrons and protons need to be small with maximized transverse overlap. Recombination rates of ions with electrons in the electron cooler can provide signals that can be used to tune the energies and transverse overlap to the required conditions. In this paper we take a close look at various detection methods for recombination processes that may be used to approach cooling.

INTRODUCTION

Low energy operation of RHIC is of particular interest to study the location of a possible critical point in the QCD phase diagram [1–4]. The performance of RHIC at energies equal to or lower than 10 GeV/nucleon is limited by nonlinearities, intra-beam scattering (IBS) processes and space-charge effects. To successfully address the luminosity and ion store lifetime limitations imposed by IBS the method of electron cooling has been envisaged. During electron cooling processes electrons are injected along with the ion beam at the nominal ion bunch velocities. The velocity spread of the ion beam is reduced in all planes through Coulomb interactions between the cold electron beam and the ion beam. The electron cooling system under construction for RHIC will be the first of its kind to use bunched beams for the delivery of the electron bunches [5–10].

Alignment of the ion and electron beams as well as the matching of the velocities between both bunches is crucial to deliver the desired cooling efficiencies. The electron cooling force greatly decreases for increasing relative energy deviation between both beams. However, direct measurements of the absolute energy of the electron beam will be challenging and are predicted to be accurate up to 10^{-3}. Monitoring of recombination rates in the electron cooler can be a viable cooling detector. Recombination rates of ions with electrons are less sensitive to energy mismatch than cooling efficiencies, and can therefore function as a easier to detect signal to tune the energies in the regime of large relative energy deviation in which electron cooling is weak, $\frac{dE}{E} > 0.1\%$. Monitoring of recombination rates in the electron cooler will provide a good understanding of the beam overlap and energy mismatch of the ion and electron beams.

This paper addresses the production rates of recombined ions as well as the various methods available to monitor recombination rates and highlights the challenges left for recombination monitors for Low Energy RHIC operations.

RADIATIVE RECOMBINATION IN THE ELECTRON COOLER

A small portion of the fully stripped gold ions will recombine with electrons in the electron cooler through radiative recombination processes. This will result in a population of non-fully stripped hydrogen-like gold ions (Au^{78+}) that propagate in the accelerator [11–14]. Estimates of recombination rates and beam lifetimes as a function of the relative beam velocities of the ion and electron bunch are calculated following the descriptions in [11]. The capture cross section in the ion rest frame for an electron is given to good approximation by [11],

$$\sigma = A\left(\frac{h\nu_0}{E}\right)\left[\ln\sqrt{\frac{h\nu_0}{E}} + \gamma_1 + \gamma_2\left(\frac{E}{h\nu_0}\right)^{\frac{1}{3}}\right] \qquad (1)$$

where E is the electron kinetic energy, h is the Planck constant, $A = \frac{4}{3\sqrt{3}\pi}\frac{he^2}{\epsilon_0 m_e^2 c^3} = 2.11\cdot10^{-22}\,\mathrm{cm}^2$, $h\nu_0 = 13.6Z^2\,eV$ is the ground state binding energy and $\gamma_1 = 0.1402$ and $\gamma_2 = 0.525$ are constants. The capture cross section may be expressed as a function of the transverse and longitudinal electron velocities by using $E = \frac{1}{2}m_e(v_\parallel^2 + v_\perp^2)$, where m_e is the electron mass and $v_\perp$ and $v_\parallel$ are the particle velocities perpendicular and parallel to the bunch velocity in the ion rest frame. The recombination rate coefficient α_r is then obtained by integration over the velocity distributions and the cross section.

$$\alpha_r = \int d^3v_1 \int d^3v_2 f_e(\mathbf{v}_1) f_I(\mathbf{v}_2)|\mathbf{v}_1 - \mathbf{v}_2|\sigma(|\mathbf{v}_1 - \mathbf{v}_2|), \qquad (2)$$

where $f_e(\mathbf{v})d^3v$ is the number of electrons in the velocity space volume d^3v and similarly for the ions. Since $\mathbf{v}_1$ and $\mathbf{v}_2$ both have gaussian distributions $\mathbf{v}_{rel} = \mathbf{v}_1 - \mathbf{v}_2$ has a gaussian distribution. Some care is needed near $\mathbf{v}_{rel} = 0$ to treat the singularity correctly.

* Work supported by Brookhaven Science Associates, LLC under Contract No. DE-AC02-98CH10886 with the U.S. Department of Energy.

ISBN 978-3-95450-147-2

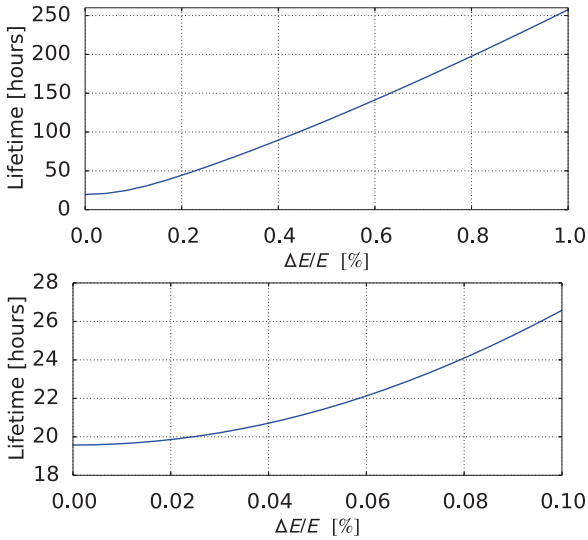

Figure 1: Lifetime of ions at large energy deviations $\frac{dE}{E} < 1.0\%$ (top) and small energy deviations $\frac{dE}{E} < 0.1\%$ (bottom). The obtained lifetime is linear in the region of interest for recombination detection.

The beam lifetime as a result of the recombination process in the cooling section is obtained from,

$$\tau = \frac{\gamma^2}{n_{eff}\alpha_r\eta} \tag{3}$$

where $\eta = \frac{l_e}{C}$, the fraction of the accelerator length occupied by the electron cooler, γ is the Lorentz factor, and where effective electron density is given by,

$$n_{eff} = \frac{\xi N_e}{(2\pi)^{\frac{3}{2}}\sigma_{e,z}^2\sigma_{e,s}} \tag{4}$$

where $\sigma_{e,s}$ is the longitudinal RMS bunch lengths of the electron bunches, $\sigma_{e,z}$ is the transverse RMS size of the electron bunches, and ξ is the geometrical longitudinal overlap between the 30 electron bunches and the ion bunch.

The ion lifetimes calculated using Eq. (3) are presented in Fig. 1. The bottom plot shows the lifetimes for relative energies $\frac{dE}{E} < 0.1\%$, while the top plot shows the lifetimes extended to larger relative energy deviations, $\frac{dE}{E} < 1\%$. The lifetime dependency at large relative energies is almost linear and will provide a proper measurable to tune the electron bunch energies.

SCHOTTKY MONITOR

The Schottky monitor has been studied as a possible detector to measure Au^{78+} using the change in revolution frequency. Generally, the change in revolution frequency is dependent on the change in circumference and the change in momentum. It is important to note, however, that the ions subject to recombination will have an unchanged velocity and therefore an unchanged momentum. In the process of capturing one electron, the ion velocity does not change. Its momentum will therefore only increase due to the additional electron mass, which is negligible at this level. The change in revolution frequency of Au^{78+} is therefore only dependent on the change in circumference due to the decreased charge. Furthermore, as the momentum is unchanged the recombined ions will not leave the bucket. Previous assumptions that recombined ions would leak into the abort gap and could be kicked resonantly are therefore dismissed [8].

The frequency shift is determined from the momentum compaction factor $\alpha_c = 1/\gamma_T^2$ and the charge difference of the Au^{78+} ions [15], and is $\frac{\Delta f}{f} = -2.4 \cdot 10^{-5}$. The acceptance of the bucket is given by frequency spread of the unrecombined ions according to

$$\sigma_f = -\left(\frac{1}{\gamma_T^2} - \frac{1}{\gamma^2}\right)\delta = 2.9 \cdot 10^{-5} \tag{5}$$

It may be concluded that the revolution frequency of the recombined gold ions will be within the frequency spread and will therefore not be detectable using the Schottky monitor. However, the Schottky monitor is still foreseen to be used for direct detection of electron cooling at energy deviations of $\frac{dE}{E} < 0.1\%$ [16] [8].

LATTICE WITH LARGE DISPERSION

A closed orbit separation between the Au^{78+} orbit and Au^{79+} orbit can be created in large dispersive regions, assuming β-functions remain small. The Au^{78+} beam may then be captured and monitored, which would also directly function as integrator of the particle population. Due to the low energy operations the transitional jump (γ_T) quadrupoles can be used to create a dispersion wave.

RHIC contains eight γ_T quadrupoles per arc used to adjust the transition energy with dispersion deviations. Four of these quadrupoles are located near the arc centers in large dispersive sections and are powered together, while the others are located in pairs at the ends of the arcs where the dispersion is smaller and share another power supply. The current powering scheme combined with an unfavorable phase advance between the cells of 83° puts considerable constraints on finding a lattice with large local dispersion without β- and dispersion wave leakage.

As both beams have independent cryostats in the arcs, it is not necessary to find a point with large dispersion and small β-function that works for both beams at the same location. Both cryostats will have to be opened, and the locations of these interventions can be independent for both beams.

Attempts to find a lattice with large local dispersion and a small β function in the arcs were unsuccessful using the current power scheme of the γ_T quadrupoles. A large local dispersion bump was created in the arc between IP12 and IP2 for both beams using an alternate powering scheme of the γ_T quadrupoles by powering them in pairs. With this new powering setup and using the trim coils (TQ4, TQ5, TQ6) as well as, depending on the beam, the 8^{th} or 9^{th} focusing quadrupole of both insertion regions enclosing the arc it is possible to obtain a large enough dispersion wave in the arcs, while retaining a small β-function.

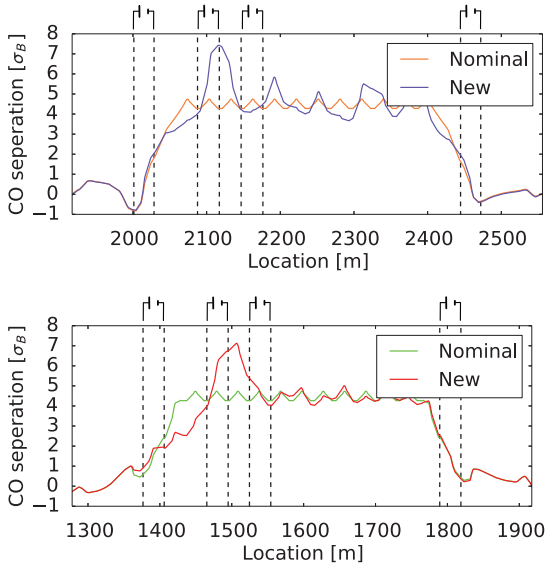

Figure 2: Closed orbit separation between the fully stripped ions and the recombined ions. The upper figure shows the separation for the Beam BLUE, while the lower figure shows the separation for Beam YELLOW for the arc between IP12 and IP2. A maximum separation of 7.4 σ_B is obtained in the BLUE Beam while, 7.0 σ_B is achieved for the YELLOW Beam. The dashed lines indicate the locations of the γ_T quadrupoles and their corresponding powering scheme.

A lattice is proposed for the blue beam that yields a maximal closed orbit separation of 7.4 σ_B. The closed orbit separation in the arc is presented in Fig. 2 (top) for the arc between IP12 and IP2. The dashed lines represent the locations of the γ_T quadrupoles and their corresponding powering scheme. There is a clear maximum of 7.4 σ_B near BI12_QD14. The new lattice has an RMS β-beating of 32% in the horizontal plane and 13% in the vertical plane in the affected arc. All optical functions distortions close at the end of the arc and do not leak into the rest of the accelerator.

A comparable lattice has been obtained for the yellow beam. These results yield a slightly smaller maximal closed orbit separation than obtained in the BLUE beam. The beam separation in the arcs is shown in Fig. 2 (bottom). At 7.0 σ_B the closed orbit separation is still large enough for the detection of recombined ions. As well as for the blue beam, the dispersion bump closes in the yellow beam. The RMS β-beating in the horizontal and vertical planes are both at 13%. Values for the quadrupole trims can be found in [10].

Detectors for Recombined Ions in the Arcs

Detection of recombined ions in the arcs can be done with several methods that are either intrusive or non-intrusive. Non-intrusive detection consists of driving the beam of Au^{78+} into the physical wall. The ions will be lost in the wall thereby creating showers of secondary particles that can be detected outside the cryostat using pin diodes. This method has been successfully used before at high energies to detect recombined copper from bound free pair production [17]. Tests to date showed a usable signal at the injection energy. The sensitivity may be improved by increasing the number of pin diodes and correctly aiming them at the source of Au^{78+} losses.

Installing a collimator inside the cryostat to capture the recombined ions would localize the losses to a single point. The created showers can then be detected outside the cryostat using pin diodes. This, however, requires breaking open the cryostat to install the collimator. Another intrusive detection method consists of designing a roman pot detector that can insert a detector directly inside the beam pipe. This is the most direct way to detect the recombined ions, but also the most demanding method. A roman pot detector would have to be designed that fits inside the arcs, where space is limited.

CONCLUSIONS

Monitoring of recombination rates will provide a secondary tuning tool to approach optimal electron cooling conditions. Detection of the change in revolution frequency between the fully stripped ions and the recombined ions using the Schottky system will not be possible. The change in revolution frequency is $2.4 \cdot 10^{-5}$ and is smaller than the frequency spread of the main ion beam $\sigma_f = 2.9 \cdot 10^{-5}$. This signal will therefore not be discernible in the schottky spectrum.

Furthermore, the momentum of the ions does not change during the radiative recombination process. This means that the recombined ions will not leave the bucket into the abort gap. As such, the particles can not be extracted through resonant kicking in the abort gap.

A lattice was found with increased dispersion in the arc between IP12 and IP2 to create a closed orbit separation between the two ion populations. A separation of 7.4 σ_B and 7.0 σ_B was found for respectively the BLUE and YELLOW beam. These separations are sufficiently large to only detect Au^{78+} ions. The recombined ions can be lost in the beam pipe at a specific location. The produced showers can then be detected using aimed pin diodes located outside the cryostat. Tests will be performed in the present RHIC run to determine the feasibility of this method. Detection may be improved by installing a collimator in the arc, or by designing a roman pot style detector to insert a detector in the beam pipe. These methods, however, require breaking open the cryostats and are therefore less desirable.

REFERENCES

[1] M. Stephanov, K. Rajagopal, and E. Shuryak. Signatures of the tricritical point in qcd. *Phys. Rev. Lett.*, 81:4816–4819, Nov 1998.

[2] Can we discover qcd critical point at RHIC? BNL, March 2006. RIKEN BNL Research Center Report No. BNL-75692-2006.

[3] A. Cho. Scheme for Boiling Nuclear Matter Gathers Steam at Accelerator Lab. *Science*, 312:190–191, 2006.

ISBN 978-3-95450-147-2

[4] G S F Stephans. critrhic: the rhic low energy program. *Journal of Physics G: Nuclear and Particle Physics*, 32(12):S447, 2006.

[5] A.V. Fedotov *et al.* Electron cooling simulations for low-energy rhic operation. In *Proceedings COOL 2007, Bad Kreuznach, Germany*, 2007.

[6] A.V. Fedotov *et al.* Electron cooling for low-energy rhic program. In *Proceedings COOL 2009, Lanzhou, China*, 2009.

[7] D.M. Gassner *et al.* Instrumentation for the proposed low energy rhic electron cooling project. In *Proceedings IBIC 2013, Oxford, UK*, 2013.

[8] D.M. Gassner *et al.* Instrumentation for the proposed low energy rhic electron cooling project with energy recovery. In *Proceedings IBIC 2014, Monterey, CA, USA*, 2014.

[9] A.V. Fedotov *et al.* Bunched beam electron cooling for low energy rhic operation. In *ICFA BD Newsletter No. 65*, page 22, 2014.

[10] F. Carlier, M. Blaskiewicz, A. Drees, A. Fedotov, W. Fischer, M. Minty, C. Montag, G. Robert-Demolaize, and P. Thieberger. Detectors for low energy electron cooling in rhic. Technical Report C-A/AP/557, BNL, Upton (USA), 2016.

[11] M Bell and John Stewart Bell. Capture of cooling electrons by cool protons. *Part. Accel.*, 12(CERN-TH-3054):49–52. 10 p, Mar 1981.

[12] A. Wolf, G. Gwinner, J. Linkemann, A. A. Saghiri, M. Schmitt, D. Schwalm, M. Grieser, M. Beutelspacher, T. Bartsch, C. Brandau, A. Hoffknecht, A. Müller, S. Schippers, O. Uwira, and D. W. Savin. Recombination in electron coolers. *Nuclear Instruments and Methods in Physics Research A*, 441:183–190, February 2000.

[13] A.B. Kuznetsov, I.N. Meshkov, and A.V. Philippov. Radiative recombination of ions and nuclei in electron cooling systems. *Physics of Particles and Nuclei Letters*, 9(4-5):346–351, 2012.

[14] W. Shi, S. Böhm, C. Böhme, C. Brandau, A. Hoffknecht, S. Kieslich, S. Schippers, A. Müller, C. Kozhuharov, F. Bosch, B. Franzke, P.H. Mokler, M. Steck, Th. Stöhlker, and Z. Stachura. Recombination of u 92 + ions with electrons. *The European Physical Journal D - Atomic, Molecular, Optical and Plasma Physics*, 15(2):145–154, 2001.

[15] S Y Lee. *Accelerator physics; 3rd ed.* World Scientific, Singapore, 2012.

[16] J M Brennan, M Blaskiewicz, P Cameron, and J Wei. Observations of Schottky Signals in RHIC and their Potential for Stochastic Cooling. 2002.

[17] R. Bruce, J. M. Jowett, S. Gilardoni, A. Drees, W. Fischer, S. Tepikian, and S. R. Klein. Observations of beam losses due to bound-free pair production in a heavy-ion collider. *Phys. Rev. Lett.*, 99:144801, Oct 2007.